

Proton Structure from a Soft-Wall Holographic QCD Model: Mass Spectrum, Form Factors, and Mechanical Properties

Jiali Deng* and Defu Hou

*Institute of Particle Physics and Key Laboratory of Quark and Lepton Physics (MOS),
Central China Normal University, Wuhan 430079, China*

(Dated: May 26, 2026)

Understanding the internal structure of the proton—including its mass spectrum, electromagnetic and gravitational form factors, and mechanical properties—remains a central challenge in hadronic physics. While lattice QCD and experimental measurements provide valuable insights, a holographic framework with a single parameter set capable of simultaneously describing these diverse observables is still lacking. Here, we employ the soft wall model, a phenomenological holographic approach that incorporates gluon condensation and linear confinement, to compute the proton mass spectrum, electromagnetic form factors (EMFFs), and gravitational form factors (GFFs). Our results show good agreement with recent experimental data and lattice QCD calculations. Despite its phenomenological nature, the model’s ability to simultaneously describe multiple observables suggests that it effectively mimics some key QCD features.

I. INTRODUCTION

What constitutes the mass and spatial extent of a proton? This deceptively simple question lies at the heart of one of the most profound challenges in modern physics: understanding the non-perturbative structure of hadrons governed by Quantum Chromodynamics (QCD). As the primary building block of visible matter, the proton’s internal dynamics—dictated by the complex interplay of confined quarks and gluons—elude a complete analytical description from first principles. Resolving this puzzle is not merely an academic pursuit but is fundamental to advancing our comprehension of nuclear physics, astrophysical phenomena, and the Standard Model itself. A comprehensive mapping of the proton’s properties, including its mass spectrum, electromagnetic and gravitational form factors (GFFs), and charge radii, provides critical windows into this sub-femtometer domain. These observables encode information on the spatial distribution of energy, momentum, and stress within the proton, thereby elucidating the mechanics that govern its interactions and stability [1–3].

Traditional lattice QCD simulations have made significant strides in computing static hadronic properties from the discretized QCD Lagrangian. However, extracting real-time dynamical processes and form factors at low momentum transfer remains computationally intensive and often limited by systematic uncertainties. Similarly, while perturbative QCD is highly successful in describing high-energy scattering, it fails in the non-perturbative regime where the coupling constant becomes large. This gap in our calculational toolkit has spurred the development of alternative non-perturbative frameworks. In this non-perturbative frontier, holographic QCD has emerged as a powerful complementary framework. Rooted in the anti-de Sitter/Conformal Field Theory (AdS/CFT) correspondence, it posits a duality between a strongly cou-

pled gauge theory in four dimensions and a classical gravitational theory in a higher-dimensional curved spacetime [4–6]. Although the original correspondence was formulated for a maximally supersymmetric, conformal gauge theory, its conceptual and mathematical toolkit has been successfully adapted, through various phenomenological models, to approximate key features of real-world QCD, such as confinement and chiral symmetry breaking [7–10]. These “bottom-up” holographic models, particularly the soft-wall model, provide a tractable geometric language to calculate hadronic properties that are notoriously difficult to access via lattice QCD or other first-principles methods, making them invaluable for generating testable predictions and conceptual insights.

Significant progress has been made using these approaches. The proton’s mass spectrum, a foundational benchmark, has been computed within various holographic and other theoretical frameworks, establishing a baseline for model calibration [11–14]. Similarly, electromagnetic form factors—the Dirac (F_1) and Pauli (F_2) form factors—which encode the spatial distributions of the proton’s charge and magnetization [15, 16], have been extensively studied both experimentally via elastic electron-proton scattering [17–19] and theoretically within holography [20–23]. These form factors provide critical, but incomplete, information about the proton’s static structure.

A more comprehensive picture requires the gravitational form factors (GFFs), which describe the proton’s coupling to the energy-momentum tensor (EMT). These form factors are of paramount importance as they reveal the origins of the proton’s mass and spin, and map its internal distributions of energy, pressure, and shear forces [3, 24]. They address the so-called “proton mass and spin crises” by quantifying how these quantum numbers are partitioned among quarks and gluons. While analogous in concept to electromagnetic form factors—probing gravitational rather than electromagnetic interactions—GFFs are far more challenging to access experimentally. Pioneering calculations for mesons and the nucleon have been performed in holographic QCD [25–29], providing

* djl2022010355@mails.ccnu.edu.cn, houdf@mail.ccnu.edu.cn

theoretical benchmarks and highlighting the rich mechanical structure hidden within the proton.

Despite these advances, a gap remains in the literature. Existing holographic studies often treat the proton's spectrum, electromagnetic structure, and gravitational structure in isolation or within different model variants. A holographic calculation that simultaneously reproduces the proton's mass spectrum, electromagnetic and gravitational form factors has not yet been presented. Such an integrated analysis provides a useful check on the consistency and descriptive capacity of a given holographic model, by testing whether a single set of calibrated parameters can describe a range of proton properties.

In this work, we employ a phenomenological holographic model with a single parameter set, which incorporates key QCD features like linear Regge trajectories and gluon condensation, to analyze the proton's structure. Our specific objectives are: (1) to compute the proton's mass spectrum within this model and determine its fundamental parameters; (2) to calculate the proton's electromagnetic form factors and the corresponding charge/magnetic radii; (3) to derive the gravitational form factors and mechanical properties.

The remainder of this paper is structured as follows. Section II introduces the soft-wall holographic QCD framework and details the calculation of the proton mass spectrum. Section III presents the computation of the proton's electromagnetic form factors. The gravitational form factors are derived and analyzed in Section IV. Finally, Section V summarizes our key findings and discusses their broader implications.

II. MASS SPECTRUM FOR PROTON

The metric of five-dimensional AdS spacetime is given by

$$ds^2 = g_{mn}dx^m dx^n = \frac{1}{z^2}(\eta_{\mu\nu}dx^\mu dx^\nu - dz^2), \quad (1)$$

where $\eta_{\mu\nu} = \text{diag}(1, -1, -1, -1)$ and $\mu, \nu = 0, 1, 2, 3$. The fifth-dimensional coordinate z extends from $z \rightarrow 0$ (the ultraviolet/UV boundary) to $z \rightarrow \infty$ (the infrared/IR boundary).

In the holographic framework, the proton is described by a dual massive spinor field propagating in five-dimensional anti-de Sitter (AdS) space. The corresponding action for this spinor field is given by [20]

$$S = \int d^4x dz \sqrt{g} e^{-\Phi(z)} \left(\frac{i}{2} \bar{\Psi} e_A^N \Gamma^A D_N \Psi - \frac{i}{2} (D_N \Psi)^\dagger \Gamma^0 e_A^N \Gamma^A \Psi - (m_5 + \Phi(z)) \bar{\Psi} \Psi \right), \quad (2)$$

where $e_A^N = z \delta_A^N$ represents the inverse vielbein, $D_N = \partial_N + \frac{1}{8} \omega_N^{ab} [\Gamma_a, \Gamma_b] - iV_N$ denotes the covariant derivative and m_5 represents the five dimensional mass of the proton. The Dirac gamma matrices $\Gamma^A = (\gamma^\mu, -i\gamma^5)$ satisfy

the Clifford algebra: $\gamma^a \gamma^b + \gamma^b \gamma^a = 2\eta^{ab}$. ω_N^{ab} represents the spin connection:

$$\omega_N^{ab} = e_M^a \partial_N e^{bM} + e_M^a \Gamma_{NP}^M e^{bP}. \quad (3)$$

We take the dilaton field in the form of [30]

$$\Phi(z) = k_1^2 z^2 \tanh(k_2^4 z^2 / k_1^2). \quad (4)$$

In this formulation, the dilaton field exhibits the following behavior at the UV boundary:

$$\Phi(z) = k_2^4 z^4, \quad (5)$$

and corresponds holographically to the dimension-4 gauge-invariant gluon condensate in the boundary field theory, while at IR boundary takes the following form

$$\Phi(z) = k_1^2 z^2. \quad (6)$$

This form gives rise to linear confinement.

The equation of motion for the spinor field is given by

$$[i e_A^N \Gamma^A D_N - \frac{i}{2} \partial_N \Phi(z) e_A^N \Gamma^A - (m_5 + \Phi(z))] \Psi = 0. \quad (7)$$

The spinor field is decomposed into left-handed and right-handed components:

$$\Psi(x^\mu, z) = \left(\frac{1 + \gamma^5}{2} \chi_R(z) + \frac{1 - \gamma^5}{2} \chi_L(z) \right) \Psi_{(4)}(x^\mu), \quad (8)$$

where $\Psi_{(4)}(x^\mu)$ satisfies the four-dimensional Dirac equation. By setting $\chi_{R/L}(z) = e^{-2A(z) + \Phi(z)/2} \varphi_{R/L}(z)$ and combining with the equation of motion, we obtain

$$-\varphi_{R/L}''(z) + [(m_5 + \Phi(z))^2 e^{2A(z)} \pm ((m_5 + \Phi(z))A'(z) + \Phi'(z)) e^{A(z)}] \varphi_{R/L}(z) = M_n^2 \varphi_{R/L}(z), \quad (9)$$

where M_n represents the mass spectrum of the proton in four-dimensional spacetime, with the quantum number $n = 1$ denoting to the ground state and $n = 2, 3, \dots$ corresponding the excited states. The wave functions satisfy the renormalization condition:

$$\int \varphi_R^{(n)}(z) \varphi_R^{(m)}(z) dz = \int \varphi_L^{(n)}(z) \varphi_L^{(m)}(z) dz = \delta_{mn}. \quad (10)$$

We obtain the mass spectrum of the proton by numerically solving the equation with Dirichlet boundary conditions, with the three parameters $k_1 = 0.450$ GeV, $k_2 = 0.333$ GeV, and $m_5 = 1.2$, which are determined by fitting the mass spectrum. In the standard AdS/CFT duality, the five-dimensional mass of the proton is $m_5 = 5/2$ as a combination of three free quarks. However, QCD is a non-conformal theory of strong interactions, so the five-dimensional mass needs to be corrected by incorporating the anomalous dimension γ [31]. The five-dimensional mass used here is the effective value that takes into account the interactions.

	Proton	$M_{\text{exp}}/\text{GeV}$	SW/GeV	Our/GeV	%M
n=1	N(939)	0.938	0.987	0.936	0.21
n=2	N(1440)	1.36 to 1.38	1.264	1.366	0.31
n=3	N(1710)	1.68 to 1.72	1.531	1.663	2.17
n=4	N(1880)	1.82 to 1.9	1.791	1.903	2.33
n=5	N(2100)	2.05 to 2.15	2.046	2.112	0.58
n=6	N(2300)	2.30	2.296	2.301	0.05

TABLE I. Comparison of the proton resonance mass spectrum between experimental values [32], results from Ref. [13] (SW), and our calculations (Our), showing agreement with relative errors below 2.5%.

As demonstrated in Table I, our calculated values show good agreement with experimental measurements, generally maintaining a deviation within 2.5%. In Ref. [13], the confinement characteristics of QCD were modeled by introducing an auxiliary correction factor to the AdS_5 metric, while our model incorporates a dilaton field in the action to address both QCD confinement and gluon condensation. This leads to a gravitational background that offers a somewhat closer description of QCD compared to the framework in Ref. [13], and yields results for the proton mass spectrum that are reasonably consistent with experimental data.

III. ELECTROMAGNETIC FORM FACTORS

In elastic scattering processes (depicted in Fig. 1), electrons and protons interact through the exchange of a virtual photon characterized by the four-momentum transfer squared q^2 . The virtual photon in this case interacts with the nucleon's constituent partons while maintaining the nucleon's integrity. Consequently, the final state preserves the nucleon identity, with momentum transfer being the sole observable change.

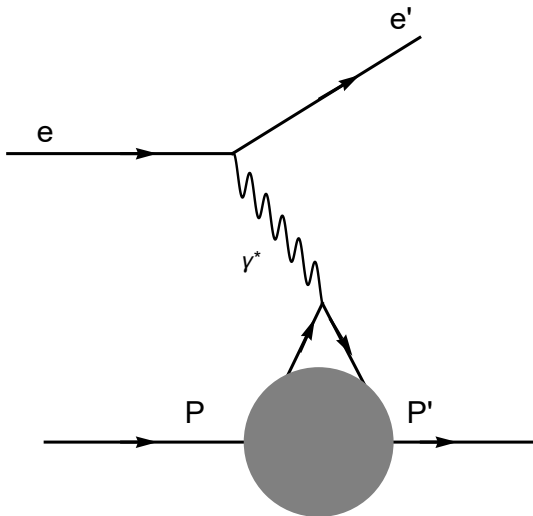


FIG. 1. Elastic electron-proton scattering mediated by virtual photon exchange [14].

The electromagnetic form factors of protons and neutrons represent fundamental nucleon observables, playing a pivotal role in elucidating nucleon structure and dynamics. The elastic electron-proton scattering process is generally characterized by two independent form factors: the Dirac form factor F_1 and the Pauli form factor F_2

$$\langle p' | J^\mu(0) | p \rangle = \bar{u}(p') [\gamma^\mu F_1(Q^2) + \frac{i\sigma^{\mu\nu} q_\nu}{2M} F_2(Q^2)] u(p), \quad (11)$$

where $\sigma^{\mu\nu} = [\gamma^\mu, \gamma^\nu]$, $q_\nu = p'_\nu - p_\nu$ is the transfer of momentum (with $q^2 = -Q^2, Q^2 > 0$), M denotes the proton mass and $J^\mu(0)$ represents the quark electromagnetic current. The Dirac form factor $F_1(Q^2)$ describes matrix elements that conserve nucleon spin, whereas the Pauli form factor $F_2(Q^2)$ mediates transitions involving spin flip. These form factors respectively characterize the spatial distributions of the nucleon's electric charge and magnetic moment.

The form of the interaction action is

$$\int d^4x dz \sqrt{-g} e^{-\Phi(z)} [\eta_1 \bar{\Psi}_{p'}(x, z) e_A^M \Gamma^A \phi_M(x, z) \Psi_p(x, z) + \eta_2 \bar{\Psi}_{p'}(x, z) e_A^M e_B^N [\Gamma^A, \Gamma^B] F_{MN}(x, z) \Psi_p(x, z)]. \quad (12)$$

where $\eta_1 = 0.5$ and $\eta_2 = 0.695$ are fixed by the constraints of charge conservation, $F_1(0) = 1$, and the experimentally measured proton magnetic moment $F_2(0) = 1.793$ respectively. The Dirac form factor is given by

$$F_1(Q^2) = \frac{1}{2} \int dz V(Q, z) (\varphi_R^2(z) + \varphi_L^2(z)) + \frac{1}{4} \eta_2 \int dz \partial_z V(Q, z) (\varphi_L^2(z) - \varphi_R^2(z)). \quad (13)$$

The Pauli form factor is given by

$$F_2(Q^2) = \eta_2 \int dz e^{-A(z)} V(Q, z) \varphi_R(z) \varphi_L(z), \quad (14)$$

where $V(Q, z)$ represents the five-dimensional electromagnetic field.

The electromagnetic field action takes the form

$$S = -\frac{1}{4} \int d^4x dz \sqrt{-g} e^{-\Phi(z)} F^{mn} F_{mn}, \quad (15)$$

where $F_{mn} = \partial_m V_n - \partial_n V_m$. The corresponding equation of motion may then be derived

$$\partial_m (\sqrt{-g} e^{-\Phi(z)} F^{mn}) = 0. \quad (16)$$

We impose the gauge condition

$$\partial_\mu V^\mu + e^{-A(z)+\Phi(z)} \partial_z (e^{A(z)-\Phi(z)} V_z) = 0. \quad (17)$$

The equation of motion consequently takes the form

$$\partial_\mu \partial^\mu V_\nu + (A'(z) - \Phi'(z)) \partial_z V_\nu + \partial_z^2 V_\nu = 0, \quad (18)$$

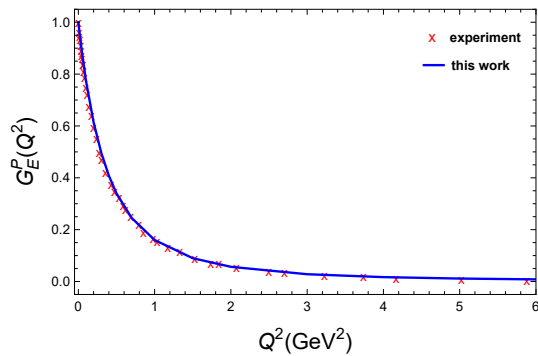


FIG. 2. The proton electric form factor $G_E^p(Q^2)$. The solid blue line is our result and the red crosses represent experimental data from Ref. [17].

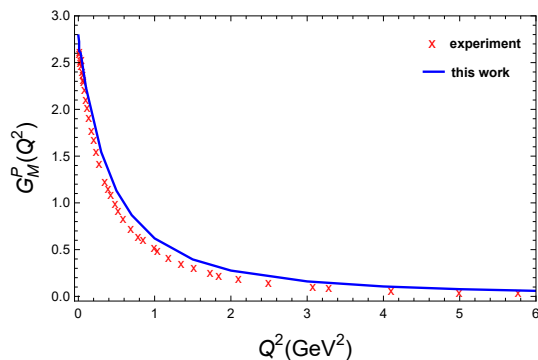


FIG. 3. The proton magnetic form factor $G_M^p(Q^2)$. The solid blue line is our result and the red crosses represent experimental data from Ref. [17].

where $V_\nu = \epsilon_\nu e^{-iqx} V(Q, z)$. At the boundary, we impose $V(Q, 0) = 1$ and implement the Neumann boundary condition in the infrared (IR) limit.

The electric and magnetic form factors can be expressed as

$$G_E(Q^2) = F_1(Q^2) - \frac{Q^2}{4M^2} F_2(Q^2), \quad (19)$$

$$G_M(Q^2) = F_1(Q^2) + F_2(Q^2). \quad (20)$$

Figure 2 and Figure 3 display the dependence of the electric and magnetic form factors on the momentum transfer Q^2 , respectively. Our calculated electric form factor is consistent with experimental measurements, while a minor deviation is observed for the magnetic form factor. This indicates that our model captures the dominant features of the proton's electromagnetic structure, though some secondary effects are not fully accounted for.

The notion of nucleon radii is fundamental to characterizing the internal architecture of protons and neutrons, offering essential insight into the nonperturbative domain of QCD. These radii are defined through multiple physical observables, each probing a distinct aspect

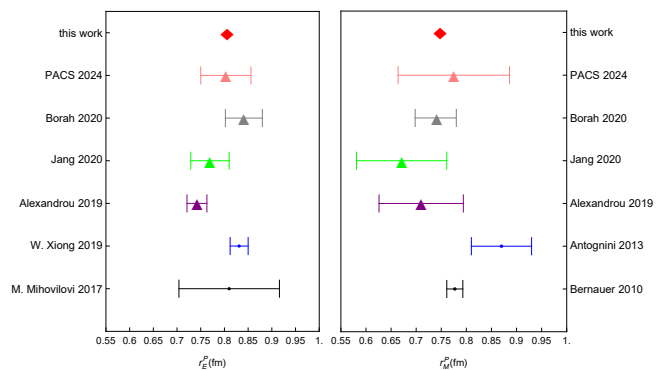


FIG. 4. A comparison of the proton's charge and magnetic radii with other models [34–37] and experiments [38–41]: the left side shows the charge radius, and the right side displays the magnetic radius.

of the nucleon's internal organization. Beyond their importance in elucidating nucleon structure, they also play a vital role in precision tests of the Standard Model. In particular, high-precision measurements of nucleon radii provide stringent constraints on theoretical approaches such as lattice QCD, chiral effective field theory, and holographic QCD.

To support our theoretical treatment, the Breit frame is adopted, with the kinematical variables Δ^ν , P^ν , and the momentum transfer squared t defined as follows [33]:

$$P^\nu = (E, \mathbf{0}), \quad \Delta^\nu = (0, \mathbf{\Delta}), \quad \Delta^2 = 4(M^2 - E^2). \quad (21)$$

The charge and magnetic radii represent key observables for probing the internal structure of nucleons. The charge radius quantifies the spatial extent of the electric charge distribution, whereas the magnetic radius characterizes the size associated with the magnetic moment, generated by the internal dynamics of quarks and gluons. The charge radius of the proton is defined as

$$\langle r_E^2 \rangle = \frac{\int d^3\mathbf{r} r^2 G_E(r)}{\int d^3\mathbf{r} G_E(r)} = 6 \frac{dG_E(Q^2)}{dQ^2} \Big|_{Q^2=0}. \quad (22)$$

The magnetic radius of the proton is defined as

$$\langle r_M^2 \rangle = \frac{\int d^3\mathbf{r} r^2 G_M(r)}{\int d^3\mathbf{r} G_M(r)} = \frac{6}{\mu} \frac{dG_M(Q^2)}{dQ^2} \Big|_{Q^2=0}, \quad (23)$$

where μ represents the magnetic moment of the proton. With $r_E^p = 0.80 fm$ and $r_M^p = 0.75 fm$, this result is relatively close to the lattice QCD result but shows a slight deviation from the experimental measurement, as shown in Figure 4.

IV. GRAVITATIONAL FORM FACTORS

The generation of the proton's mass represents one of the most fundamental challenges in QCD. Remarkably, the QCD Lagrangian contains only light quarks and massless gluons as fundamental degrees of freedom,

yet must generate the observed proton mass of approximately 0.94 GeV. A corresponding fundamental question addresses the origin of the proton's spin: although simplistic quark models attribute its spin-1/2 configuration exclusively to the intrinsic spins of valence quarks, the complete theoretical decomposition of the proton's total angular momentum continues to present an outstanding challenge in hadronic physics. To address these fundamental questions, we examine the matrix elements of the proton's energy-momentum tensor (EMT). These matrix elements provide direct access to the proton's core structural characteristics, including its mass distribution, spin composition, and internal stress profiles [3].

The general parameterization of the EMT matrix elements for the proton can be written as

$$\begin{aligned} \langle p' | T^{\mu\nu}(0) | p \rangle = & \bar{u}(p') [\gamma^{(\mu} P^{\nu)} A(Q^2) + \frac{i P^{(\mu} \sigma^{\nu)\alpha} q_\alpha}{2M} B(Q^2) \\ & + \frac{q^\mu q^\nu - \eta^{\mu\nu} q^2}{4M} D(Q^2)] u(p), \end{aligned} \quad (24)$$

where $\gamma^{(\mu} p^{\nu)} = \frac{1}{2}(\gamma^\mu p^\nu + \gamma^\nu p^\mu)$, $q^2 = (p'^\mu - p^\mu)^2 = t$, and $P^\mu = \frac{1}{2}(p^\mu + p'^\mu)$. In holographic QCD, Equation (24) serves as the source term for metric fluctuations, $\eta'_{\mu\nu} = \eta_{\mu\nu} + h_{\mu\nu}$. The gravitational form factors of the proton are obtained through the coupling between the irreducible representations of the five-dimensional graviton field $h_{\mu\nu}$ and the bulk proton field. The energy-momentum tensor of the proton can be expressed as

$$T^{\mu\nu}(x, z) = \frac{-2}{\sqrt{-g}} \frac{\delta \mathcal{L}}{\delta g_{\mu\nu}}. \quad (25)$$

Substituting the metric perturbation into the action, we obtain the interaction action for the coupling between the graviton and the proton field as

$$S_{int} = \frac{1}{2} \int d^4x dz \sqrt{-g} h_{\mu\nu} T^{\mu\nu} + o(h^2). \quad (26)$$

Substituting the perturbed metric $\eta'_{\mu\nu} = \eta_{\mu\nu} + h_{\mu\nu}$ into the gravitational action S_G , we obtain the corresponding action as

$$S_h = \frac{1}{4\kappa^2} \int d^4x dz \sqrt{-g} e^{-\Phi(z)} (\partial_\alpha h^{\mu\nu} \partial^\alpha h_{\mu\nu} - \frac{1}{2} \partial_\alpha h \partial^\alpha h). \quad (27)$$

Introduce the harmonic-traceless gauge $\partial_\lambda h^\lambda_\alpha = \partial_\alpha h = 0$. Under this gauge condition, with $h = h^\mu_\mu$ denoting the trace and κ as the Newton constant, the graviton satisfies the equation of motion given by Eq. 27:

$$\partial_\alpha [\sqrt{-g} e^{-\Phi(z)} g^{\alpha\lambda} \partial_\lambda h_{\mu\nu}] = 0. \quad (28)$$

This can then be simplified to

$$(\partial_z^2 + (3A'(z) - \Phi'(z))\partial_z - Q^2)h(Q^2, z) = 0, \quad (29)$$

With the ansatz $h_{\mu\nu} = \epsilon_{\mu\nu} e^{-iq_G x} h(Q^2, z)$, $q_G^2 = -Q^2$, we impose the following boundary conditions on $h(Q^2, z)$:

$$h(Q^2, 0) = h(0, z) = 1, \quad \partial_z h(Q^2, \infty) = 0. \quad (30)$$

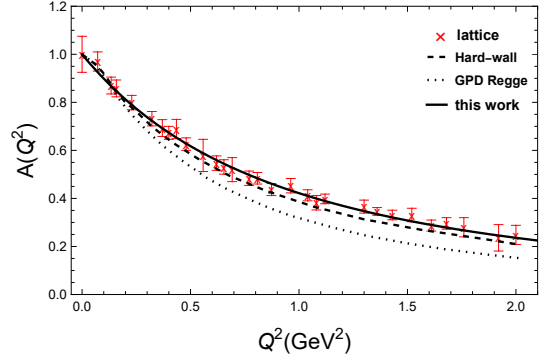


FIG. 5. The proton GFF $A(Q^2)$. The red crosses represent the lattice results at $\mu^2 = 4 \text{ GeV}^2$ [27], the dotted and dashed lines denote the predictions from other models [20, 42], and the solid black line is our result.

From the above analysis, we can obtain

$$A(Q^2) = \frac{1}{2} \int dz h(Q^2, z) (\varphi_L^2(z) + \varphi_R^2(z)). \quad (31)$$

Figure 5 shows the dependence of the gravitational form factor A on the squared momentum transfer Q^2 . Our results are consistent with the lattice results. This suggests that our model is capable of describing the energy-momentum distribution of the proton.

In our holographic model, the Pauli-like form factor satisfies $B(Q^2) = 0$ because the coupling of the graviton to the proton's spin connection vanishes. Furthermore, the dynamics of the gravitational form factor $D(Q^2)$ is not included in the holographic model, making it impossible for us to compute $D(Q^2)$ directly. Next, by combining the perturbative asymptotic form of the gravitational form factor $D(Q^2)$ and the proton's mass radius and mechanical radius as inputs, we phenomenologically determine the form of the gravitational form factor $D(Q^2)$.

The asymptotic form of the proton's gravitational form factor at large Q^2 , from pQCD [43, 44], is

$$A(Q^2) \sim \frac{\alpha^2(Q^2)}{Q^4}, \quad D(Q^2) \sim -\frac{\alpha^2(Q^2)}{Q^6}, \quad (32)$$

According to Eq. (31), we assume that the gravitational form factor $D(Q^2)$ takes the form

$$D(Q^2) = -\frac{D(0)}{1 + \lambda Q^2} A(Q^2), \quad (33)$$

where $D(0)$ and λ are determined by the proton's mass radius and mechanical radius, respectively.

The energy, pressure, and shear force distributions within the proton are expressed in terms of combinations of its gravitational form factors in the following [33]:

$$\epsilon(r) = M[A(Q^2) + \frac{Q^2}{4M^2}(A(Q^2) - 2J(Q^2) + D(Q^2))]_{FT}. \quad (34)$$

$$p(r) = \frac{1}{6M} \frac{1}{r^2} \frac{d}{dr} (r^2 \frac{d}{dr} [D(Q^2)]_{FT}). \quad (35)$$

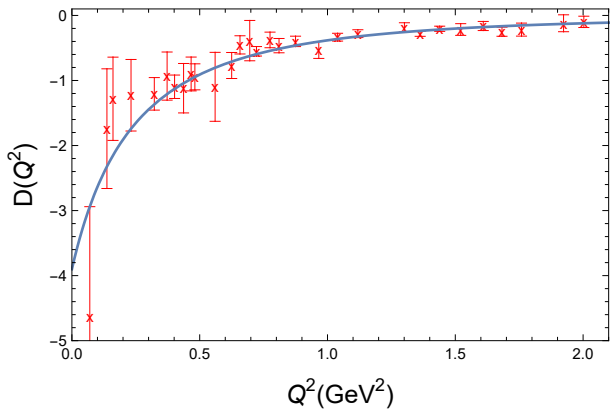


FIG. 6. The proton GFF $D(Q^2)$. The red crosses represent the lattice results at $\mu^2 = 4 \text{ GeV}^2$ [27] and the solid blue line is our result.

$$s(r) = -\frac{1}{4M} r \frac{d}{dr} \left(\frac{1}{r} \frac{d}{dr} [D(Q^2)]_{FT} \right). \quad (36)$$

where FT denotes the Fourier transform and takes the form:

$$[f(r)]_{FT} = \int \frac{d^3 \Delta}{(2\pi)^3} e^{-i\Delta \cdot \mathbf{r}} f(Q^2). \quad (37)$$

The mass radius of the proton is

$$\langle r_{mass}^2 \rangle = \frac{\int d^3 \mathbf{r} r^2 \epsilon(r)}{\int d^3 \mathbf{r} \epsilon(r)} = -6 \frac{dA(Q^2)}{dQ^2} \Big|_{Q^2=0} - \frac{3D(0)}{2M^2}. \quad (38)$$

The longitudinal force is given in terms of p and s as:

$$F_{||}(r) = p(r) + \frac{2}{3} s(r), \quad (39)$$

where it represents the normal force per unit area. Local stability requires the longitudinal force to be positive ($F_{||}(r) > 0$), indicating an outward direction; otherwise, the proton would undergo collapse. Similarly, in stable hydrostatic systems, the shear force is generally positive, satisfying $s(r) > 0$ and thereby providing a second condition for local stability. The mechanical radius of the proton is

$$\langle r_{mech}^2 \rangle = \frac{\int d^3 \mathbf{r} r^2 F_{||}(r)}{\int d^3 \mathbf{r} F_{||}(r)} = \frac{6D(0)}{\int_{\infty}^0 D(t) dt}. \quad (40)$$

The average values of the theoretical results [45] are $r_{mass} \approx 0.73 \text{ fm}$, and $r_{mech} \approx 0.75 \text{ fm}$, yielding $D(0) \approx 3.9$ and $\lambda = 3.3$. This value of $D(0)$ is consistent with lattice fits.

Figure 6 shows the dependence of the gravitational form factor D on the squared momentum transfer Q^2 . Our results are in basic agreement with lattice calculations. This result supports our assumption about the relation between the two form factors based on the perturbative asymptotic form.

By substituting the obtained gravitational form factors into Equations (34)–(36) and (39), we obtain the energy,

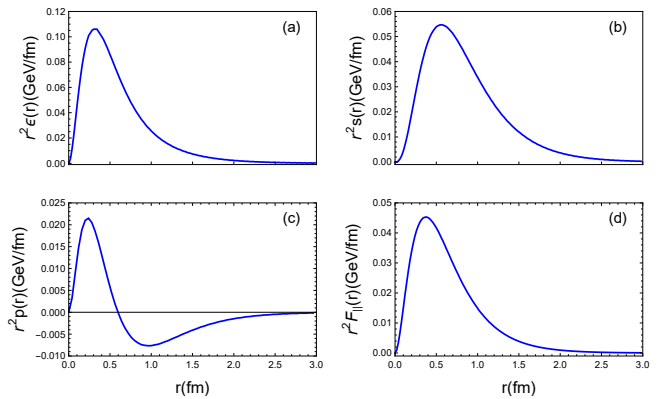


FIG. 7. Spatial distributions of the weighted (a) energy density $r^2 \epsilon(r)$, (b) pressure $r^2 p(r)$, (c) shear force $r^2 s(r)$, and (d) longitudinal force $r^2 F_{||}(r)$ inside the proton.

pressure, shear, and longitudinal force distributions of the proton, as presented in Figs. 7.

Our calculations satisfy the energy conservation and mechanical equilibrium conditions:

$$M = \int d^3 \mathbf{r} \epsilon(r), \quad \int dr r^2 p(r) = 0. \quad (41)$$

As shown in Fig. 7, panel (a) represents the weighted energy density, which has a peak at $r \approx 0.31 \text{ fm}$, and its integral satisfies the energy conservation (Eq. 41). Panel (b) represents the weighted pressure. Unlike the weighted energy density, which remains positive throughout, the weighted pressure distribution exhibits a sign change at approximately $r = 0.59 \text{ fm}$. The positive pressure peaks at $r = 0.23 \text{ fm}$, while the negative pressure reaches its maximum magnitude at about $r = 0.93 \text{ fm}$. The pressure adheres to the von Laue condition in Eq. (41), where the outward push from the positive region is balanced by the inward pull from the negative region, thereby ensuring the proton's mechanical stability. The positive pressure occupies a compact core, whereas the negative pressure spreads out over an extended periphery. Panel (c) represents the weighted shear force, which has a peak at $r \approx 0.55 \text{ fm}$ and reflects the internal stress anisotropy of the proton. Panel (d) represents the weighted longitudinal force, which has a peak at $r \approx 0.36 \text{ fm}$ and is directly related to the local force balance. The relationship between the longitudinal force, the pressure, and the shear force is discussed in Eq. 39.

In this section, we first predict the proton's gravitational form factor $A(Q^2)$ from the previous model, and the results are consistent with lattice calculations. Since our model does not incorporate the dynamics of the gravitational form factors $B(Q^2)$ and $D(Q^2)$, we set $B(Q^2) = 0$, which is also consistent with lattice calculations indicating that this term is very small. Combined with the asymptotic form from perturbative theory, we assume a parametrization for $D(Q^2)$ and take the mean square radius from different theoretical models as inputs. We then obtain the complete gravitational form factor

$D(Q^2)$ as well as the relation between these two form factors. Our results are consistent with lattice calculations. Finally, using the gravitational form factors as inputs, we investigate four different mechanical quantities inside the proton.

V. CONCLUSION

In the study of proton structure, we employ a soft-wall model that incorporates a dilaton field $\Phi(z) = k_1^2 z^2 \tanh(k_2^4 z^2 / k_1^2)$. This model breaks conformal symmetry in the low-energy region to generate confinement effects and simulates gluon condensation in the high-energy region, thereby more closely approximating the actual behavior of quantum chromodynamics compared to the traditional $\Phi(z) = k_3^2 z^2$ -type soft-wall model. In this work, we investigate the proton structure by calculating the mass spectrum, electromagnetic form factors, electromagnetic radius, and gravitational form factors. Using these gravitational form factors as input, we then obtain the mechanical properties of the proton.

We begin by calculating the proton mass spectrum using a Schrödinger-like equation incorporating anomalous dimensions. The results exhibit a deviation of less than 3% from experimental data, demonstrating good consistency.

Subsequently, using the same parameters, we predict the electromagnetic form factors, electromagnetic radius, and gravitational form factor $A(Q^2)$ of the proton. These predictions are found to be consistent with experimental measurements and lattice calculations.

Next, since the dynamics of the gravitational form factor $D(Q^2)$ are not included in the holographic model, making it impossible for us to compute $D(Q^2)$ directly, we phenomenologically determine $D(Q^2)$ by combining its perturbative asymptotic form with the proton's mass radius and mechanical radius—both taken as the average values from different theoretical models—as inputs. Our result is consistent with lattice calculations. Finally, with the gravitational form factors thus obtained, we compute the distribution of mechanical properties of the proton.

Although the results are encouraging, it is essential to acknowledge several limitations of this study. For instance, some discrepancies remain between our calculated magnetic form factor and electromagnetic radius and the corresponding experimental measurements. Future research should aim to clarify these discrepancies and explore the long-term implications of our findings. Furthermore, applying this framework to study other hadrons and their interactions may contribute to a deeper understanding within the broader context of quantum chromodynamics.

In summary, the results obtained from our model are generally consistent with both lattice calculations and experimental measurements. Our results show that a relatively simple phenomenological holographic model—with its parameters determined by the proton mass spectrum—is able to predict the electromagnetic form factors, the electromagnetic radius, and the gravitational form factor $A(Q^2)$ that are in basic agreement with experimental data and lattice results. Furthermore, although our calculation of $D(Q^2)$ is not a rigorous derivation, combining the perturbative asymptotic form with radius inputs yields a gravitational form factor $D(Q^2)$ that is in basic agreement with lattice results, and we also obtain the relation between the two gravitational form factors. These findings offer some useful perspectives for future theoretical studies of the proton's internal structure.

ACKNOWLEDGMENTS

We thank Hai-cang Ren and Yan-Qing Zhao for useful discussions. This work is supported in part by the National Key Research and Development Program of China under Contract No. 2022YFA1604900. This work is also partly supported by the National Natural Science Foundation of China (NSFC) under Grants No. 12435009, and No. 12275104.

REFERENCES

-
- [1] M. Guidal, H. Moutarde, and M. Vanderhaeghen, Generalized Parton Distributions in the valence region from Deeply Virtual Compton Scattering, *Rept. Prog. Phys.* **76**, 066202 (2013), [arXiv:1303.6600 \[hep-ph\]](#).
 - [2] O. V. Selyugin, Models of parton distributions and the description of form factors of nucleon, *Phys. Rev. D* **89**, 093007 (2014), [arXiv:1404.2702 \[hep-ph\]](#).
 - [3] V. D. Burkert, L. Elouadrhiri, F. X. Girod, C. Lorcé, P. Schweitzer, and P. E. Shanahan, Colloquium: Gravitational form factors of the proton, *Rev. Mod. Phys.* **95**, 041002 (2023), [arXiv:2303.08347 \[hep-ph\]](#).
 - [4] J. M. Maldacena, The Large N limit of superconformal field theories and supergravity, *Adv. Theor. Math. Phys.* **2**, 231 (1998), [arXiv:hep-th/9711200](#).
 - [5] E. Witten, Anti de Sitter space and holography, *Adv. Theor. Math. Phys.* **2**, 253 (1998), [arXiv:hep-th/9802150](#).
 - [6] O. Aharony, S. S. Gubser, J. M. Maldacena, H. Ooguri, and Y. Oz, Large N field theories, string theory and gravity, *Phys. Rept.* **323**, 183 (2000), [arXiv:hep-th/9905111](#).
 - [7] J. Polchinski and M. J. Strassler, Hard scattering and gauge / string duality, *Phys. Rev. Lett.* **88**, 031601 (2002), [arXiv:hep-th/0109174](#).
 - [8] A. Karch, E. Katz, D. T. Son, and M. A. Stephanov, Linear confinement and AdS/QCD, *Phys. Rev. D* **74**, 015005 (2006), [arXiv:hep-ph/0602229](#).

- [9] J. Deng and S.-Q. Feng, Holographic deconfined QGP phase diagram and entropy with an anomalous flow in a magnetic field background, *Phys. Rev. D* **105**, 026015 (2022), arXiv:2109.10103 [hep-ph].
- [10] S. He, M. Huang, Q.-S. Yan, and Y. Yang, Confront Holographic QCD with Regge Trajectories, *Eur. Phys. J. C* **66**, 187 (2010), arXiv:0710.0988 [hep-ph].
- [11] G. F. de Teramond and S. J. Brodsky, Hadronic spectrum of a holographic dual of QCD, *Phys. Rev. Lett.* **94**, 201601 (2005), arXiv:hep-th/0501022.
- [12] S. J. Brodsky, G. F. de Teramond, H. G. Dosch, and J. Erlich, Light-Front Holographic QCD and Emerging Confinement, *Phys. Rept.* **584**, 1 (2015), arXiv:1407.8131 [hep-ph].
- [13] E. Folco Capossoli, M. A. Martín Contreras, D. Li, A. Vega, and H. Boschi-Filho, Hadronic spectra from deformed AdS backgrounds, *Chin. Phys. C* **44**, 064104 (2020), arXiv:1903.06269 [hep-ph].
- [14] J. Deng and D. Hou, Nucleon structure from an AdS/QCD model in the Veneziano limit, *Phys. Rev. D* **112**, 036011 (2025), arXiv:2502.00771 [nucl-th].
- [15] S. Pacetti, R. Baldini Ferroli, and E. Tomasi-Gustafsson, Proton electromagnetic form factors: Basic notions, present achievements and future perspectives, *Phys. Rept.* **550-551**, 1 (2015).
- [16] V. Punjabi, C. F. Perdrisat, M. K. Jones, E. J. Brash, and C. E. Carlson, The Structure of the Nucleon: Elastic Electromagnetic Form Factors, *Eur. Phys. J. A* **51**, 79 (2015), arXiv:1503.01452 [nucl-ex].
- [17] J. Arrington, W. Melnitchouk, and J. A. Tjon, Global analysis of proton elastic form factor data with two-photon exchange corrections, *Phys. Rev. C* **76**, 035205 (2007), arXiv:0707.1861 [nucl-ex].
- [18] A. J. R. Puckett *et al.*, Final Analysis of Proton Form Factor Ratio Data at $Q^2 = 4.0, 4.8$ and 5.6 GeV^2 , *Phys. Rev. C* **85**, 045203 (2012), arXiv:1102.5737 [nucl-ex].
- [19] W. Xiong and C. Peng, Proton Electric Charge Radius from Lepton Scattering, *Universe* **9**, 182 (2023), arXiv:2302.13818 [nucl-ex].
- [20] Z. Abidin and C. E. Carlson, Nucleon electromagnetic and gravitational form factors from holography, *Phys. Rev. D* **79**, 115003 (2009), arXiv:0903.4818 [hep-ph].
- [21] R. S. Sufian, G. F. de Teramond, S. J. Brodsky, A. Deur, and H. G. Dosch, Analysis of nucleon electromagnetic form factors from light-front holographic QCD : The spacelike region, *Phys. Rev. D* **95**, 014011 (2017), arXiv:1609.06688 [hep-ph].
- [22] K. A. Mamo and I. Zahed, Electromagnetic radii of the nucleon in soft-wall holographic QCD, *Nucl. Phys. B* **997**, 116388 (2023), arXiv:2106.00752 [hep-ph].
- [23] M. Ahmady, D. Chakrabarti, C. Mondal, and R. Sandapen, Nucleon electroweak form factors using spin-improved holographic light-front wavefunctions, *Nucl. Phys. A* **1016**, 122334 (2021), arXiv:2105.02213 [hep-ph].
- [24] S. J. Brodsky, D. S. Hwang, B.-Q. Ma, and I. Schmidt, Light cone representation of the spin and orbital angular momentum of relativistic composite systems, *Nucl. Phys. B* **593**, 311 (2001), arXiv:hep-th/0003082.
- [25] Z. Abidin and C. E. Carlson, Gravitational form factors of vector mesons in an AdS/QCD model, *Phys. Rev. D* **77**, 095007 (2008), arXiv:0801.3839 [hep-ph].
- [26] K. A. Mamo and I. Zahed, Nucleon mass radii and distribution: Holographic QCD, Lattice QCD and GlueX data, *Phys. Rev. D* **103**, 094010 (2021), arXiv:2103.03186 [hep-ph].
- [27] D. C. Hackett, D. A. Pefkou, and P. E. Shanahan, Gravitational Form Factors of the Proton from Lattice QCD, *Phys. Rev. Lett.* **132**, 251904 (2024), arXiv:2310.08484 [hep-lat].
- [28] S. Nair, C. Mondal, S. Xu, X. Zhao, A. Mukherjee, and J. P. Vary (BLFQ), Gravitational form factors and mechanical properties of quarks in protons: A basis light-front quantization approach, *Phys. Rev. D* **110**, 056027 (2024), arXiv:2403.11702 [hep-ph].
- [29] Z. Dehghan, F. Almaksusi, and K. Azizi, Mechanical properties of proton using flavor-decomposed gravitational form factors, *JHEP* **06**, 025, arXiv:2502.16689 [hep-ph].
- [30] D. Li and M. Huang, Dynamical holographic QCD model for glueball and light meson spectra, *JHEP* **11**, 088, arXiv:1303.6929 [hep-ph].
- [31] E. Folco Capossoli, M. A. Martín Contreras, D. Li, A. Vega, and H. Boschi-Filho, Proton structure functions from an AdS/QCD model with a deformed background, *Phys. Rev. D* **102**, 086004 (2020), arXiv:2007.09283 [hep-ph].
- [32] S. Navas *et al.* (Particle Data Group), Review of particle physics, *Phys. Rev. D* **110**, 030001 (2024).
- [33] M. V. Polyakov and P. Schweitzer, Forces inside hadrons: pressure, surface tension, mechanical radius, and all that, *Int. J. Mod. Phys. A* **33**, 1830025 (2018), arXiv:1805.06596 [hep-ph].
- [34] R. Tsuji, Y. Aoki, K.-I. Ishikawa, Y. Kuramashi, S. Sasaki, K. Sato, E. Shintani, H. Watanabe, and T. Yamazaki (PACS), Nucleon form factors in $N_f=2+1$ lattice QCD at the physical point: Finite lattice spacing effect on the root-mean-square radii, *Phys. Rev. D* **109**, 094505 (2024), arXiv:2311.10345 [hep-lat].
- [35] K. Borah, R. J. Hill, G. Lee, and O. Tomalak, Parametrization and applications of the low- Q^2 nucleon vector form factors, *Phys. Rev. D* **102**, 074012 (2020), arXiv:2003.13640 [hep-ph].
- [36] Y.-C. Jang, R. Gupta, H.-W. Lin, B. Yoon, and T. Bhattacharya, Nucleon electromagnetic form factors in the continuum limit from $(2+1+1)$ -flavor lattice QCD, *Phys. Rev. D* **101**, 014507 (2020), arXiv:1906.07217 [hep-lat].
- [37] C. Alexandrou, S. Bacchio, M. Constantinou, J. Finkenrath, K. Hadjiyiannakou, K. Jansen, G. Koutsou, and A. Vaquero Aviles-Casco, Proton and neutron electromagnetic form factors from lattice QCD, *Phys. Rev. D* **100**, 014509 (2019), arXiv:1812.10311 [hep-lat].
- [38] M. Mihovilović *et al.*, First measurement of proton's charge form factor at very low Q^2 with initial state radiation, *Phys. Lett. B* **771**, 194 (2017), arXiv:1612.06707 [nucl-ex].
- [39] W. Xiong *et al.*, A small proton charge radius from an electron-proton scattering experiment, *Nature* **575**, 147 (2019).
- [40] J. C. Bernauer *et al.* (A1), High-precision determination of the electric and magnetic form factors of the proton, *Phys. Rev. Lett.* **105**, 242001 (2010), arXiv:1007.5076 [nucl-ex].
- [41] A. Antognini *et al.*, Proton Structure from the Measurement of $2S - 2P$ Transition Frequencies of Muonic Hydrogen, *Science* **339**, 417 (2013).
- [42] M. Guidal, M. V. Polyakov, A. V. Radyushkin, and M. Vanderhaeghen, Nucleon form-factors from generalized parton distributions, *Phys. Rev. D* **72**, 054013 (2005), arXiv:hep-ph/0410251.

- [43] X.-B. Tong, J.-P. Ma, and F. Yuan, Perturbative calculations of gravitational form factors at large momentum transfer, *JHEP* **10**, 046, [arXiv:2203.13493 \[hep-ph\]](#).
- [44] E. Ruiz Arriola and W. Broniowski, Particle seismology: mechanical and gravitational properties from parton-hadron duality, in *65. Jubilee Cracow School of Theoretical Physics: Fundamental Interactions – 65 years of the Cracow School* (2026) [arXiv:2604.26537 \[hep-ph\]](#).
- [45] M. Goharipour, F. Irani, M. H. Amiri, H. Fatehi, B. Falahi, A. Moradi, and K. Azizi (MMGPDs), Can we determine the exact size of the nucleon?: A comprehensive study of different radii, *Nucl. Phys. B* **1017**, 116962 (2025), [arXiv:2503.08847 \[hep-ph\]](#).